

A NEW PROBE OF THE PLANET-FORMING REGION IN T TAURI DISKS

EDWIN BERGIN¹ AND NURIA CALVET², MICHAEL L. SITKO^{3,10}, HERVE ABGRALL⁴, PAOLA D'ALESSIO⁵, GREGORY J. HERCZEG⁶, EVELYNE ROUEFF⁴, CHUNHUA QI², DAVID K. LYNCH^{7,10}, RAY W. RUSSELL^{7,10}, SUELLEN M. BRAFFORD^{8,10}, R. BRAD PERRY^{9,10}

Accepted by the Astrophysical Journal Letters

ABSTRACT

We present new observations of the FUV (1100-2200 Å) radiation field and the near- to mid-IR (3–13.5 μm) spectral energy distribution (SED) of a sample of T Tauri stars selected on the basis of bright molecular disks (GM Aur, DM Tau, LkCa15). In each source we find evidence for Ly α induced H₂ fluorescence and an additional source of FUV continuum emission below 1700 Å. Comparison of the FUV spectra to a model of H₂ excitation suggests that the strong continuum emission is due to electron impact excitation of H₂. The ultimate source of this excitation is likely X-ray irradiation which creates hot photo-electrons mixed in the molecular layer. Analysis of the SED of each object finds the presence of inner disk gaps with sizes of a few AU in each of these young (~1 Myr) stellar systems. We propose that the presence of strong H₂ continuum emission and inner disk clearing are related by the increased penetration power of high energy photons in gas rich regions with low grain opacity.

Subject headings: accretion, accretion disks—astrobiology—astrochemistry — circumstellar matter — stars: pre-main sequence — ultraviolet:stars

1. INTRODUCTION

In recent years there has been growing evidence for evolution of solid particles in young (≤ 10 Myr) proto-planetary accretion disks (Beckwith, Henning, & Nakagawa 2000; D'Alessio 2003, and references therein). The onset of this evolution lies in the coagulation of sub-micron sized particles into larger grains; a process which continues until the larger grains decouple from the gas and settle to a dusty mid-plane. In the mid-plane these solid particles grow in size until they become large enough to gravitationally focus collisions with smaller bodies, eventually making planets (Safronov 1972; Weidenschilling 1997).

Since dust grains within the disk absorb stellar UV and optical photons and re-emit at wavelengths longer than $\gtrsim 2\mu\text{m}$, the dust evolutionary process has direct consequences on disk continuum emission. Thus, at early evolutionary stages the presence of dust in the inner disk ($\lesssim 10$ AU) is revealed by optically thick emission at near and mid-infrared (IR) wavelengths. As grains grow the opacity at these wavelengths decreases, revealing stellar photospheric emission. The formation of giant planets can also affect the dust emission. Gravitational inter-

action between the disk and the forming planet results in the formation of a gap as the mass of the planet increases (Bryden et al. 1999; Alibert, Mordasini & Benz 2004 and references therein), producing a significant decrease in disk flux in the near-IR (Rice et al. 2003, R03).

What is less recognized, at least in terms of an observational signature, is that the molecular evolution is closely linked with the dust evolution. Disks in a more advanced degree of dust evolution will be more easily permeated by the destructive short-wavelength radiation fields generated in part by accretion. Since grain evolution and planet formation proceeds more rapidly in the denser inner disk (Weidenschilling 1997), these effects will be magnified in the very regions that are closest to the source(s) of radiation. In this *Letter* we suggest that a strong H₂ UV emission feature is an observational consequence of grain growth/planet formation in the inner disks of young ($\sim 10^6$ yr) accreting T Tauri disks.

2. OBSERVATIONS

The sources chosen for the STIS UV study are DM Tau, GM Aur, and LkCa 15. In Table 1 we provide some basic characteristics for these systems. All sources have relatively similar properties and were selected on the basis of the presence of gas disks with rich molecular complexity (Koerner, Sargent, & Beckwith 1993; Dutrey, Guilloteau, & Guelin 1997; Qi et al. 2003). Each are single star systems with no evidence for binary companions (White & Ghez 2001). HST/STIS spectra of DM Tau, LkCa 15, and GM Aur were obtained for HST program G09374 on Feb. 5, Feb. 13, and Apr. 1, 2003 respectively. Exposures were taken using the G140L (1150 Å – 1730 Å) and G230L (1570 Å – 3180 Å) gratings with an aperture size of 2". The spectral resolution per pixel for G140L is $\Delta\lambda = 0.6$ Å and $\Delta\lambda = 1.58$ Å for G230L. With a FWHM of the PSF of 1.5 pix at the FUV and 2 pix at the NUV, this results in effective resolutions of 0.9 Å ($R\sim 1550$) at the FUV and 3

¹ University of Michigan, 825 Dennison Building, 501 E. University Ave., Ann Arbor, MI 48109-1090; email: ebergin@umich.edu

² Harvard-Smithsonian Center for Astrophysics, 60 Garden St., Cambridge, MA 02138

³ Department of Physics, University of Cincinnati, Cincinnati OH 45221-0011

⁴ LUTH, UMR 8102 du CNRS, Observatoire de Paris, Section de Meudon, Place Jules Janssen, 92195 Meudon, France

⁵ Instituto de Astronomía, UNAM, Apartado Postal 72-3 (Xan-gari), 58089 Morelia, Michoacan, Mexico; México

⁶ JILA, University of Colorado, Boulder, CO 80309-0440

⁷ The Aerospace Corporation, Los Angeles, CA 90009

⁸ School of Law, University of Dayton, Dayton, OH 45469-2760

⁹ NASA Langley Research Center

¹⁰ Visiting Astronomer, NASA Infrared Telescope Facility, operated by the University of Hawaii under contract with the National Aeronautics and Space Administration.

Å in the NUV ($R \sim 770$). The plate scale is $0.024''$ per pixel in both FUV and NUV, so the aperture size is large enough for spectrophotometry. Exposure times were 10m (G230L) and ~ 65 m (G140L) for DM Tau and GM Aur and 189m (G140L) and 37m (G230L) for LkCa 15. Standard CALSTIS pipeline procedures were used to reduce the data.¹

The targets were observed in the mid-IR over the course of three separate observing runs (Jan. & Feb. 2003) that overlapped the HST observations for DM Tau and LkCa 15 (5-6 week difference for GM Aur). Observations were obtained with the Aerospace Corporation’s Broadband Array Spectrograph System (BASS; Sitko, Lynch, & Russell 2000) with a $3.4''$ beam on the NASA Infrared Telescope Facility. This instrument uses a cold beam-splitter to separate the light into two separate wavelength regimes ($2.9\text{--}6\ \mu\text{m}$; $6\text{--}13.5\ \mu\text{m}$). Each beam is dispersed onto a 58-element Blocked Impurity Band linear array, thus allowing for simultaneous coverage from $2.9\text{--}13.5\ \mu\text{m}$. The spectral resolution is wavelength-dependent, ranging from $R \sim 30$ to 125 over each wavelength region. Integration times were 40 min (GM Aur), 227 min (DM Tau), and 143 min (LkCa15). All observations are calibrated relative to α Tau, with typical airmasses ~ 1.07 and calibrator airmasses ranging from 1.03–1.12.

3. RESULTS

3.1. UV Spectra of T Tauri Stars

Figure 1 shows the FUV de-reddened fluxes of the T Tauri stars in our sample including the spectra of TW Hya from Herczeg et al. (2002). In Table 1 we provide the strength of the FUV radiation at 100 AU (estimated by integrating the FUV radiation field from 1100 to 1700 Å) normalized to that of the interstellar UV radiation field. This estimate is a lower limit due to the unknown Ly α flux.²

Figure 2 shows the spectrum of LkCa15 with prominent emission features identified. In TW Hya (Figure 1) there is a strong Ly α emission line that is not as evident in the other sources, because these sources are embedded within molecular clouds; in contrast TW Hya has no local cloud and little interstellar absorption (Herczeg et al. 2004). Evidence for strong Ly α radiation that penetrates to the molecular layer can be inferred from the presence of numerous emission features coincident with Ly α pumped H₂ emission lines. In Figure 2 some of these coincidences are denoted for LkCa 15, but similar features are seen in all sources shown in our sample. Beyond the clear H₂ emission line features there also appears a sharp rise in emission below 1700 Å. This feature is likely due to a combination of *discrete and continuum* emission emitted by H₂ molecules in excited electronic states.

¹ There is some overlap in wavelength coverage between the NUV and FUV detectors. No correction was needed to be applied to match flux levels, and the data is presented with overlap included. Some data was not shown at the short wavelength end of the NUV spectra to better illustrate particular features. However, the NUV data in this spectral region closely mirrors the FUV data.

² There is little information of the strength of the radiation field below 1100 Å. FUSE data of TW Hya indicates that the FUV field strength, $G_0 = 3400$ (including Ly α), does not change appreciably with this radiation included (Herczeg et al. 2004).

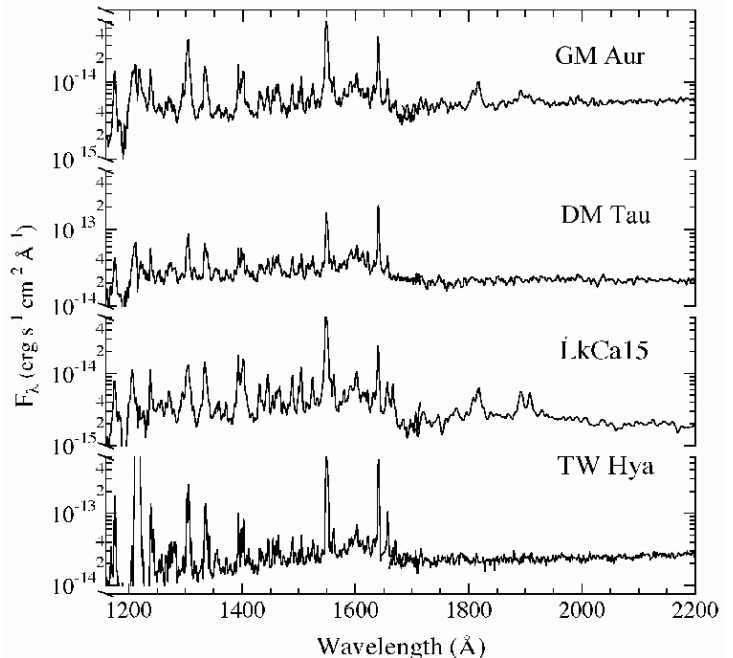


FIG. 1.— HST/STIS spectra of objects in our sample, including the spectra of TW Hya first discussed in Herczeg et al. (2002), but with reduced spectral resolution ($1.5\ \text{\AA}$).

H₂ emission below 1700 Å can result from at least two physical mechanisms (cf. Herczeg et al. 2004), Ly α induced fluorescence and electron impact excitation followed by fluorescence (Liu et al. 2002). Ly α excitation involves only the ungerade electronic states ($B\ ^1\Sigma_u$ and $C\ ^1\Pi_u$), producing a spectrum permeated by discrete emission lines with some continuum emission. However, electron impact excitation can also excite the gerade states (E, F etc.) which cascade toward the B, C states and emit subsequent UV fluorescence. This produces a broader spectrum with greater contribution from the H₂ dissociation continuum (Abgrall et al. 1997; Jonin et al. 2000; Liu et al. 2003). A model spectrum for 100eV electron impact spectrum is displayed in Figure 2. A simple comparison of our data to the electron impact model in Figure 2 shows similarities that are suggestive that electron impact excitation may be important.³ The implications of this result are discussed in §4.

3.2. Spectral Energy Distributions

The targets, selected on the basis of strong disk molecular emission, show indications of significant dust evolution in their inner disks. For example, the $K-L$ colors of LkCa 15 and GM Aur are bluer than 86% of the Taurus sample (consisting of 51 CTTS with near and mid-IR observations from Kenyon & Hartmann 1995, KH95), and the $K-L$ color of DM Tau is bluer than 70% of the sample. The BASS observations of the targets strengthen these indications. In Figure 3, we compare the mid-IR, optical, and IRAS data of the targets to the median SED of Classical T Tauri stars in Taurus from D’Alessio et al.

³ In the electron impact model there is an additional strong feature near 1200 Å which we do not discuss due to the close proximity of Ly α . In a future publication we will compare the FUV spectra with H₂ excitation models in greater detail.

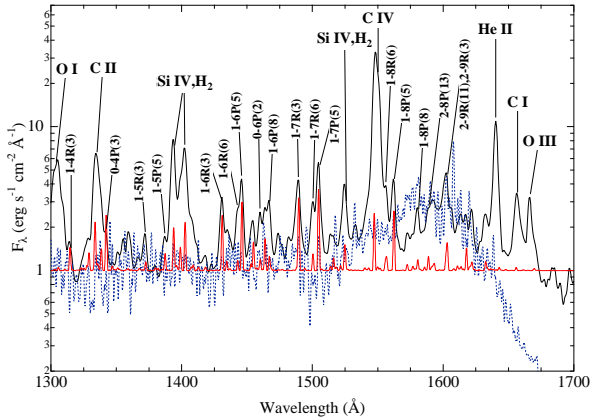


FIG. 2.— Comparison of observed LkCa15 spectrum (solid black line), with strong features identified, the electron impact model spectrum (dotted blue line), and model of Ly α fluorescence (solid red line). The model spectra were produced using an excitation model and molecular transition probabilities in the discrete and continuum range (Abgrall, Roueff, & Drira 1994, 2000). For ease in comparison, the fluxes from both observation and models are normalized to the flux at 1425 Å.

(1999). The SEDs of the targets show a clear flux deficit in the near-IR relative to the median in Taurus, analogous to that of TW Hya (cf. Figure 3), for which inner disk clearing due to the action of a planet opening a gap in the disk has been suggested (§1; C02; R03).

Attempting to get insight into the structure of the inner region, we use a simple model, following C02 and Uchida et al. (2004). The model consists of: (1) A vertical “wall” in the inner edge of the outer disk, representing the far edge of the gap. This wall, located at radius R_t with height z_w is frontally illuminated by the star and emits as a black body with temperature T_w , where $T_w = T_{eff}/R_t^{1/2}/2^{1/4}$ (cf. C02). We are ignoring effects of geometry of the gap, inclination, and occultation.⁴ (2) An optically thin inner disk, extending from the dust destruction radius to R_t , with optical depth τ_{min} at $10 \mu\text{m}$. This region has a mixture of small ($\sim 0.1\mu\text{m}$) and large ($\sim 2\mu\text{m}$) grains, and we have added organics and troilite to the mostly amorphous silicate grains of Uchida et al. (2004). The optically thin dust temperatures are calculated from radiative equilibrium at each radius. The results of this simple modeling procedure are shown in Figure 3, where we show the spectrum of each individual component; model parameters are given in Table 1. It is clear, in the case of LkCa 15, the two components alone cannot account for the excess emission above photospheric fluxes in the near IR; some excess can be seen in the case of GM Aur and DM Tau as well. We find that this excess can be explained by black body emission at $T_d = 1400\text{K}$, the dust destruction temperature (see Figure 3). We suggest that the innermost region of the inner disk is optically thick and has a rim at the dust destruction radius from where this emission arises, as is the case in other young disks (Dullemond, Dominik, &

⁴ Emission from the wall in the disk is inclination dependent. However, the targets have inclinations $\sim 30 - 60^\circ$ (Simon, Dutrey, & Guilloteau 2000; Qi et al. 2003), for which the wall emission is within 50% of the maximum (Dullemond, Dominik, & Natta 2001).

Natta 2001; Muzerolle et al. 2003, M03).

Several points can be extracted from our analysis: (1) all disks have cleared their inner regions up to few AU.⁵ (2) The height of the wall z_w at R_t puts an upper limit to the height of the outer disk at that radius because the wall could be “puffed up” with the enhanced radiative heating. Comparing with predictions from disk structure calculations, the low values of z_w/R_t in GM Aur and DM Tau are consistent with models with very significant grain growth (cf. Figure 5 in D’Alessio et al. 2001); the much lower value of LkCa 15 cannot be explained by models with well mixed gas and dust; it probably requires a significant amount of dust settling. (3) The column density of dust required to produce the silicate feature is $\Sigma_d \sim \tau_{min}/\kappa(10\mu\text{m}) \sim 0.001 \text{ gr cm}^{-2}$, with $\kappa(10\mu\text{m}) \sim 1 \text{ cm}^2/\text{gr}$. Using standard expressions for accretion disks (cf. M03), we can estimate the column density of gas in the inner disk from the mass accretion rate \dot{M} . With $\dot{M} \sim 3 \times 10^{-9} M_\odot \text{ yr}^{-1}$ as representative of our objects (Table 1), we obtain $\Sigma_{gas} \sim 20 \text{ gr cm}^{-2}$ at 1 AU, for $\alpha = 0.01$, $T = 100\text{K}$, and $M = 1M_\odot$, with corresponding dust column of $\sim 0.2 \text{ gr cm}^{-2}$ (using the standard dust-to-gas mass ratio), much higher than detected. As discussed in C02, one possibility is that the remaining dust is locked up in larger bodies with low near-IR opacities. (4) We can estimate the height z_{dust} of the rim at the dust destruction radius from the solid angle required to fit the emission, assuming a cylindrical geometry. The radius of this cylinder would be the dust destruction radius, which can be calculated from the stellar and accretion luminosities (M03, Table 1). We find $z_{dust} \leq 0.1H$ (Table 1), with $H \sim 0.1R$, which is much lower than the height of the rim previously found in thick inner disks (Dullemond et al. 2001; M03). We note that black body emission alone can explain the near-IR excess (Figure 3.) This suggests that the innermost optically thick region has a small radial extent and moreover, may be in the shadow of the rim (Dullemond et al. 2001). Taken together, all these results suggest that the solids in the inner disks of the targets have experienced significant evolution.

4. DISCUSSION

In a small sample of stars selected solely on the basis of strong and diverse disk molecular emission we have found two striking results (1) the presence of strong UV continuum emission from H_2 molecules and (2) evidence for grain growth and possible inner disk clearing by planetary bodies. Although our sample is limited we suggest that these two results may be related. The process of grain growth and inner disk clearing will certainly enhance the penetration power of both UV and X-ray radiation, perhaps even leading to regions that are optically thin to UV radiation with penetration only weakly limited by molecular opacity. The direct or improved exposure of molecular gas to high energy radiation can certainly produce the H_2 UV emission features seen in our study, which only require a small molecular col-

⁵ The location of the outer edge of the gap R_t for GM Aur is larger than that inferred by Rice et al. (2003). These authors only had broad band colors, and included the silicate emission as emission from the wall. With our better observations, the optically thin emission can be separated from the wall optically thick emission, which is much lower in the $\sim 10\mu\text{m}$ region.

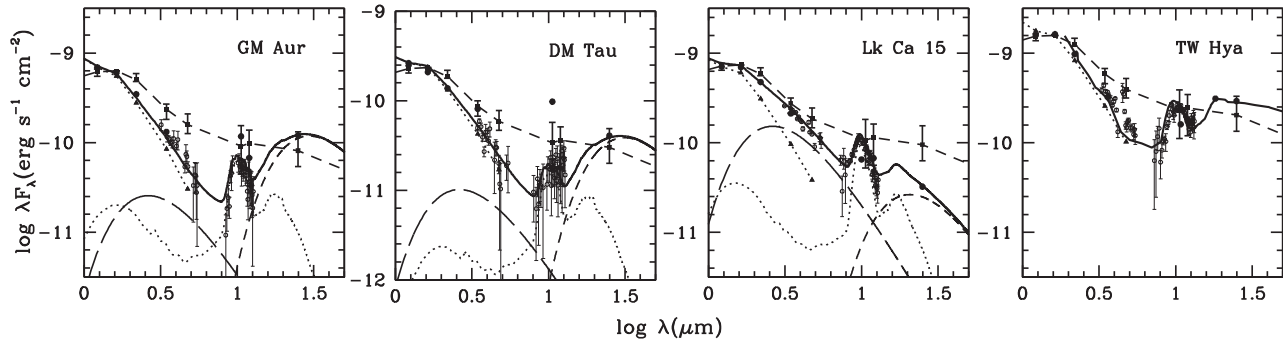


FIG. 3.— Spectral energy distributions of GM Aur, DM Tau, and LkCa 15: BASS data (small open circles), optical and IRAS bands from KH95 (large solid circles). Also shown are the photospheric fluxes (solid triangles joint by dotted line), and the contribution of the wall (short-dashed lines), the optically thin inner region (dotted line), and the possible rim at the dust destruction radius (long dashed line). We show for comparison the median of Taurus (solid rectangles joined by dashed lines, error bars denote the quartiles of the distribution) from D’Alessio et al. (1999). The last panel shows the SED of TW Hya, with data and model from Calvet et al. (2002). Photospheric fluxes are calculated from standard colors and spectral types from KH95, scaled to the de-reddened J magnitude of each object. Models discussed in §3.2 are shown in solid lines. We do not include the contribution of the outer disk, which becomes important at longer wavelengths than those considered here (C02).

TABLE 1
STELLAR PROPERTIES AND MODEL RESULTS

Stellar Properties			
	GM Aur	LkCa 15	DM Tau
SpT	K3	K5	M1
T_{eff}	4730	4350	3720
A_V	0.14	0.62	0.9
L	0.83	0.74	0.25
R_*	1.35	1.51	1.20
$\log L_{acc}$	-1.149	-1.055	-1.749
$\log \dot{M}$	-8.563	-8.096	-9.103
G_0	340	1500	240
Model Results			
R_t/AU	6.5	3	4
T_w/K	124	177	117
z_w/R	0.12	0.03	0.13
τ_{min}	0.005	0.007	0.007
R_d/R_*	12	9.8	12
z_{dust}/R_d	0.01	0.08	0.006

NOTE. — G_0 = Field at 100 AU in Habing, 1 Habing = standard UV flux from interstellar radiation field. Stellar data in solar units from Kenyon & Hartmann (1995).

umn ($< 10^{19} \text{ cm}^{-2}$; Herczeg et al. (2004)). Additional FUV spectra of young TTS combined with forthcoming Spitzer/IRS and BASS data on the mid-IR SED will be required to fully determine the relation between FUV emission and grain growth.

Electron impact excitation requires the mixture of hot electrons within an undissociated H_2 layer (Raymond, Blair, & Long 1997). For these systems we can assume that the upper layers of the inner disks are mostly cleared of small grains and H_2 self-shielding limits photo-destruction. Under normal circumstances radiation will erode the H_2 layer, but these systems are still accreting, which provides a source term. In the shielded layer some hot photo-electrons will be produced via UV ionization of C^+ , but these do not have sufficient energy ($\sim 2 \text{ eV}$) for H_2 excitation. Thus, electron excitation likely requires X-ray photons which have greater penetration power and produce higher energy electrons. In the dust poor inner

disk the opacity for abundant 1 keV X-rays will also be reduced by nearly a factor of 3 (Glassgold, Najita, & Igea 1997) allowing X-rays to penetrate into the self-shielded layer, ionize H_2 , and produce hot electrons mixed within molecular gas. The radiation produced by electron impact excitation of H_2 , therefore does not originate from the star (with an oblique angle of incidence on the disk like Ly α), but rather arises from the upper layers of the disk itself. This increases the penetration power of the UV radiation with resulting effects on disk physics (UV clearing of inner disk, accretion, gas temperature structure, etc.) and the chemistry of species sensitive to radiation below 1700 Å.

The reduction of dust opacity inside the planet forming regions of the inner disk along with the presence of gas (inferred from accretion) suggests that some of the heating mechanisms believed important for the outer disk will not be effective in the inner disk. In particular, the efficiency of photoelectric heating can be expected to be reduced and a greater role must be played by X-ray heating and UV excited H_2 collisional de-excitation. Thus the gas physics of an evolving inner disk will change as a function of dust evolution. UV emission from H_2 must trace these changes and provides a direct tracer of the gas conditions within the planet-forming regions of T Tauri disks that are only weakly probed by the dust.

We are grateful for constructive and useful comments from an anonymous referee. EAB and NC are grateful for several discussions with A. Dalgarno. This work has been supported by NASA through grant 09374.01-A from the STSCI and Origins of Solar Systems grant NAG5-9670. PD acknowledges grants from DGAPA and CONACyT. For this work MLS was supported in part by NASA grant NAG5-9475 and the University Research Council of the Univ. of Cincinnati. DKL and RWR were supported by The Aerospace Corporation’s Independent Research and Development program and by the USAF Space and Missile Systems Center through the Mission Oriented Investigation and Experimentation program, under contract F4701-00-C-0009.

REFERENCES

- Abgrall H., Roueff E., Launay F., Roncin J.-Y., 1994, *Can. J. Phys.* 72, 856
- Alibert, Y., Mordasini, C., & Benz, W. 2004, *A&A*, 417, L25
- Beckwith, S. V. W., Henning, T., & Nakagawa, Y. 2000, *Protostars and Planets IV*, eds. V. Mannings, A.P. Boss, S.S. Russell, (University of Arizona Press; Tucson), 533
- Bryden, G., Chen, X., Lin, D. N. C., Nelson, R. P., & Papaloizou, J. C. B. 1999, *ApJ*, 514, 344
- Calvet, N., D'Alessio, P., Hartmann, L., Wilner, D., Walsh, A., & Sitko, M. 2002, *ApJ*, 568, 1008 (C02)
- D'Alessio, P. 2003, *Revista Mexicana de Astronomia y Astrofisica Conference Series*, eds. M. Reyes-Ruiz and E. Vazquez-Semadeni, 18, 14
- D'Alessio, P., Calvet, N., & Hartmann, L. 2001, *ApJ*, 553, 321
- D'Alessio, P., Calvet, N., Hartmann, L., Lizano, S., & Cantó, J. 1999, *ApJ*, 527, 893
- Dullemond, C. P., Dominik, C., & Natta, A. 2001, *ApJ*, 560, 957
- Dutrey, A., Guilloteau, S., & Guelin, M. 1997, *A&A*, 317, L55
- Glassgold, A. E., Najita, J., & Igea, J. 1997, *ApJ*, 480, 344
- Herczeg, G. J., Linsky, J. L., Valenti, J. A., Johns-Krull, C. M., & Wood, B. E. 2002, *ApJ*, 572, 310
- Herczeg, G. J., Wood, B.E., Linsky, J. L., Valenti, J. A., & Johns-Krull, C. M. 2004, *ApJ*, 607, 369
- Jonin, C., Liu, X., Ajello, J. M., James, G. K., & Abgrall, H. 2000, *ApJS*, 129, 247
- Kenyon, S.J. & Hartmann, L. 1995, *ApJS*, 101,117 (KH95)
- Koerner, D. W., Sargent, A. I., & Beckwith, S. V. W. 1993, *Icarus*, 106, 2
- Liu, X., Shemansky, D. E., Abgrall, H., Roueff, E., Dziczek, D., Hansen, D. L., & Ajello, J. M. 2002, *ApJS*, 138, 229
- Liu, X., Shemansky, D. E., Abgrall, H., Roueff, E., Ahmed, S. M., & Ajello, J. M. 2003, *Journal of Physics B Atomic Molecular Physics*, 36, 173
- Muzerolle, J., Calvet, N., Hartmann, L., & D'Alessio, P. 2003, *ApJ*, 597, L149 (M03)
- Qi, C., Kessler, J. E., Koerner, D. W., Sargent, A. I., & Blake, G. A. 2003, *ApJ*, 597, 986
- Raymond, J. C., Blair, W. P., & Long, K. S. 1997, *ApJ*, 489, 314
- Rice, W. K. M., Wood, K., Armitage, P. J., Whitney, B. A., & Bjorkman, J. E. 2003, *MNRAS*, 342, 79
- Safronov, V. S. 1972, *Symposium on the Origin of the Solar System*, 89
- Simon, M., Dutrey, A., & Guilloteau, S. 2000, *ApJ*, 545, 1034
- Sitko, M. L., Lynch, D. K., & Russell, R. W. 2000, *AJ*, 120, 2609
- Uchida, K.I. et al. 2004, *ApJ* (in press)
- Weidenschilling, S. J. 1997, *Icarus*, 127, 290
- White, R. J. & Ghez, A. M. 2001, *ApJ*, 556, 265